A 3D symmetry-preserving simulation of a concentrated photovoltaic thermal (CPVT) solar collector

D Santos, J Rigola, J Castro and F X Trias

Technical University of Catalonia, Heat and Mass Transfer Technological Center (CTTC), Carrer Colom 11 Edifici TR4, Terrassa (Barcelona), Spain.

E-mail: daniel.santos.serrano@upc.edu

Abstract. In this work, a general collocated and unconditionally stable framework on unstructured meshes for solving Conjugate Heat Transfer (CHT) problems is presented by means of preserving the underlying symmetries of the continuous differential operators, thus not introducing uncontrolled artificial numerical dissipation to our system. Then, this framework is applied to solve a Concentrated PhotoVoltaic Thermal (CPVT) Solar Collector. Furthermore, a new boundary condition is implemented to consider the heat transfer between enclosed elements, including radiation. The model is validated using experimental data.

1. Introduction

Solving conjugate heat transfer problems involves a set of partial differential equations, namely, Navier-Stokes equations, mass conservation equation and energy conservation equation for fluids, heat conduction equation for solids [1] and radiative transfer equations if radiation is also present [2]. Numerical methods approximate solutions for these equations as a general solution is unknown. Finite Volume Methods are popular in fluid dynamics, and used by prominent computational fluid dynamics (CFD) codes like OpenFOAM and ANSYS-Fluent. A collocated arrangement is used by them due to its simplicity and computational efficiency [3, 4].

The integration of various disciplines, such as material physics and thermal engineering, is imperative in the field of solar cell technology. To enhance the analysis of solar cell systems and aid in the optimization process, CFD proves to be a valuable tool [5, 6]. By adopting a simulation-driven approach, we can optimize system design or evaluate performance under different conditions without the necessity of doing an experiment.

Azfali et. al. have recently proposed a zero-dimensional thermal model for a CPVT collector, which involves solving heat transfer and energy balance equations[7]. Calise et. al. introduced a finite-volume method in one dimension, which takes into account energy and mass balances, performing energetic and exergetic studies [8]. Demircan et al. utilized this model along with an electrical model to investigate the operational conditions and efficiencies of PV and CPVT systems[9].

In this regard, a 3-dimensional finite-volume transient conjugate heat transfer model, including radiation, was not found in the literature when studying CPVT systems. Such a model can provide detailed information on different aspects, such as temperature distributions,

pressure drops, and thermal efficiencies. An integrated model that can solve problems concerning conjugate heat transfer phenomena [10] along with radiation transport [11], using OpenFOAM, will be developed in this work.

Figure 1 shows a general scheme of a CPVT system:

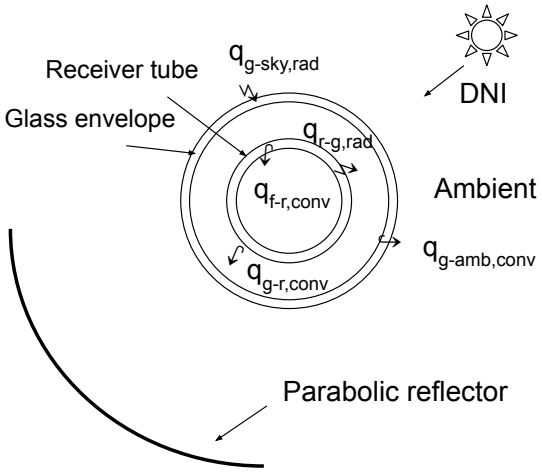

Figure 1. General diagram of the CPV-T system. Heat transfer flux exchanges are represented in the picture.

2. Numerical model and implementation

The "chtMultiRegionFoam" solver within OpenFOAM will be used to simulate the CPVT solar collector (modified to conserve symmetries of differential operators and kinetic energy and for being unconditionally stable [3, 12]). In addition, the radiative interactions will be solved using a new boundary condition within OpenFOAM. It is possible to solve the RTE at this point, but this procedure is computationally very expensive.

The (incompressible) Navier-Stokes equations for fluid parts of the system, along with the mass and energy conservation equations are:

$$\nabla \cdot \mathbf{u} = 0 \tag{1}$$

$$\frac{\partial \mathbf{u}}{\partial t} + (\mathbf{u} \cdot \nabla)\mathbf{u} = \frac{1}{\rho}\nabla(p - \rho \mathbf{g}\mathbf{z}) + \nu \nabla^2 \mathbf{u} - \mathbf{g}, \tag{2}$$

$$\frac{\partial T}{\partial t} + \mathbf{u} \cdot \nabla T = \frac{\kappa}{\rho c_p}\nabla^2 T + \mathbf{S}_t, \tag{3}$$

and conduction equation for solids:

$$\frac{\partial T}{\partial t} = \frac{\kappa}{\rho c_p}\nabla^2 T + \mathbf{S}_t, \tag{4}$$

where $\mathbf{u}$ is the velocity, p is the pressure ρ is the density, $\mathbf{g}$ is the gravity vector, z is the coordinate in which the gravity force is acting, ν is the kinematic viscosity, T is the temperature, κ is the thermal conductivity, c_p is the heat capacity and $\mathbf{S}_t$ is the source term. These equations are coupled at the solid-fluid and solid-solid interfaces, where the heat flux exiting one domain enters the adjacent domain, and the temperature is assumed to be the same.

The heat transfer is affected by natural convection in the surrounding air and forced convection between the fluid and the pipe. These convective effects play an essential role in the overall heat transfer process. It is worth noting that including the numerical resolution of

the radiative transfer equation (RTE) in the current scenario would be pretty expensive because the computational domain would increase significantly, especially when dealing with a thin glass covering. In addition, solar radiation can pass through the glass with ease, whereas thermal infrared radiation cannot. Hence, solving the equations for two radiation bands, including semi-transparent media, is essential. For this reason, a new boundary condition was implemented in OpenFOAM. This boundary condition extends the "externalWallHeatFlux" boundary condition by including radiative interactions and empirical correlations to compute the local heat transfer coefficient:

$$\kappa \nabla T = a_s q_{in} - e_t \sigma T^4 + a_t e_g \sigma T_g^4 + a_t r_g e_t \sigma T^4 + h(T_a - T), \tag{5}$$

where a_s and a_t are the solar and thermal absorptivity of the material, e_t is the thermal emissivity of the material, q_{in} is the incoming radiation, σ is the Stefan-Boltzmann constant, T is the temperature of the material, e_g is the thermal emissivity of the glass, T_g is the average temperature of the glass, r_g is the thermal reflectivity of the glass, h is the heat transfer coefficient between the material and the air, and T_a is the average temperature of the air. The first term models the incoming radiative flux, the second one models the thermal radiation emitted by the material, the third one models the absorbed thermal radiation by the material that comes from the thermal radiation emitted by the glass, the fourth term models the absorbed thermal radiation coming from the reflected thermal radiation of the material by the glass, and the last term models the convective heat exchange.

T_g and T_a temperatures are updated according to a heat balance as follows:

$$T_a^{n+1} = T_a^n + \frac{1}{\rho_a c_{p,a} V_a} \Delta t [Q_a^n + h_{in}(T_g^n - T_a^n) A_{g,in}], \tag{6}$$

$$\begin{aligned} T_g^{n+1} = T_g^n + \frac{1}{\rho_g c_{p,g} V_g} \Delta t [a_g q_r A_{g,in} + a_{s,g} q_{in} \bar{A} - e_g \sigma T_g^4 (A_{g,in} + A_{g,out}) \\ + e_g \sigma T_{sky}^4 A_{g,out} + h_{in}(T_a^n - T_g^n) A_{g,in} + h_{out}(T_{out}^n - T_g^n) A_{g,out}]. \end{aligned} \tag{7}$$

These equations are a first-order time accurate discretization of the air and glass heat balance, assuming an average temperature on both. Here, Q_a^n is computed at each time step by means of computing the (anisotropic) wall heat flux at each control volume face that is in contact with the surrounding air, q_r is the incident radiative flux, which comes from the emitted radiation of the elements inside the glass. h_{in} and h_{out} are the heat transfer coefficients computed between the glass and the inside air, and between the glass and the outside air, respectively. In equation (7), the first balance term is the incoming absorbed radiation from the elements that are inside the glass and the second balance term is the part of the solar incoming radiation absorbed by the glass (taking into account that the radiation is not incident to all the outside area of the glass, an incidence area $\bar{A}$ shall be estimated). The third balance term is the thermal radiation emitted by the glass, the fourth is the diffusive radiation coming from the surroundings, and the last is the convective heat exchange. T_{sky} and T_{out} are the sky and the outside temperatures, which can be taken as the outside temperature for enclosed rooms.

2.1. Verification and validation of the model

Simulations with various mesh sizes were performed to ensure the solution is consistent regardless of the mesh size (model verification procedure). The number of control volumes in x, y, and z directions was increased until an asymptotic solution was obtained. It is worth noting that the meshes used were non-regular, which means that the size of the control volumes was not constant. Table 1 shows that the maximum differences between Mesh D and Mesh E are below $0.2°C$ for the temperature curves. Due to the small differences between Mesh E and Mesh D and computational power requirements, Mesh E has been considered optimal for the following numerical cases.

Table 1. Number of control volumes of the tested meshes, maximum temperature differences between the tested mesh and the previous coarser one, and average temperature of the PCB. For the position of the temperature sensors s1, s2 and s3 (see figure 3)

	NCV	ΔT_{s1}	ΔT_{s2}	ΔT_{s3}	T_{PCB}
Mesh A	364000	-	-	-	76.85
Mesh B	1086000	1.14	0.72	0.51	76.84
Mesh C	1630000	0.10	0.10	0.09	76.76
Mesh D	2340000	0.36	0.26	0.22	76.35
Mesh E	3270000	0.19	0.16	0.15	76.25

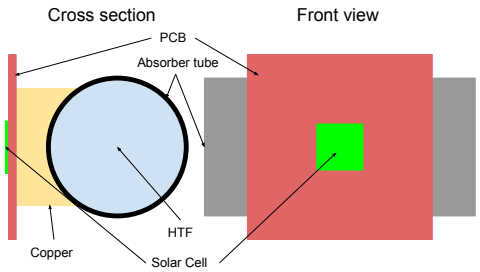

Figure 2. Cross section and front view of the receiver.

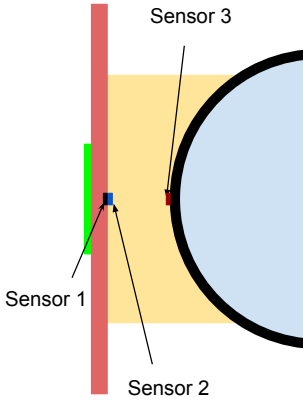

Figure 3. Position of the temperature sensors.

Figure 2 shows the main components of the system to take into account: i) an absorber pipe; ii) a printed circuit board (PCB) that has the solar cell attached; and iii) a piece made of copper that connects the PCB with the pipe. Furthermore, a light guide tunnel concentrates radiation onto the solar cell (see figure 4).

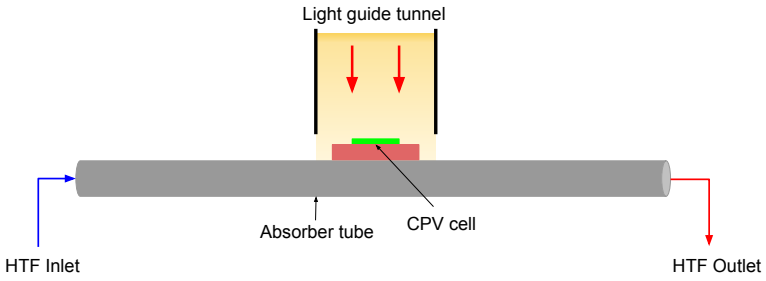

Figure 4. CPVT single solar collector experimental configuration [13]. The glass is omitted in the figure.

The radiation coming from the lamp is known a priori and dependent on time. It is added as an external irradiance to the inlet boundary. Finally, the process of converting solar radiation to electricity was modeled using a (sink) source term in the conduction equation.

The experiment consisted of 5 parts: in part 1, the lamp is turned on, while the HTF remains at constant temperature (at $65°C$); in part 2, the lamp is turned off, while the HTF remains at the same temperature; in part 3 the HTF is cooled down progressively from $65°C$ to $20°C$ without turning on the lamp; in part 4 the lamp is turned on again, while the HTF remains at $20°C$; finally, in part 5 the lamp is turned off again. The temperature data obtained experimentally in [13] is compared against the numerical results obtained for Mesh E.

Figure 5, 6 and 7 show that the numerical results are in quite good agreement with the experimental data, including the steady-state temperature, which is slightly overpredicted in part 1 and slightly underpredicted in part 4. Slightly overpredicted temperatures can also be observed during part 3, where bigger errors can be found (maximum errors are about $+1.5°C$). A possible explanation for these bigger errors can be the effect of when the lamp is turned off and when the HTF starts to cool down. The temperature is very sensitive to these effects, and a delay of these in the simulation can give overpredicted temperatures. Even so, the model could predict the system's behavior in all the parts of the experiment with precision.

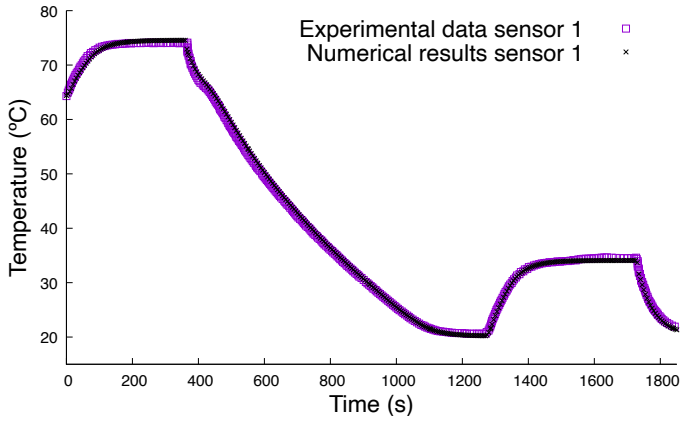

Figure 5. Comparison between the temperature obtained at the temperature sensor 1.

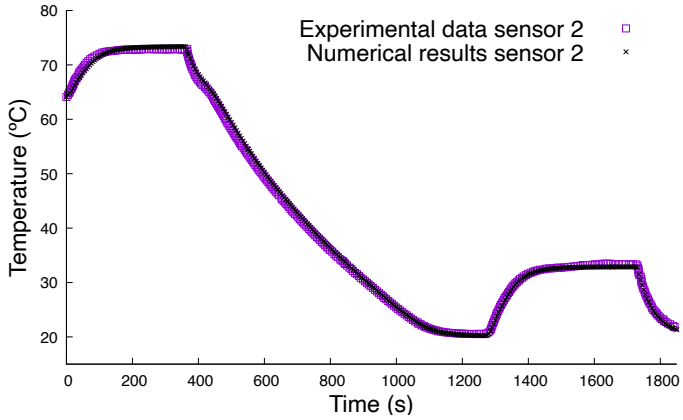

Figure 6. Comparison between the temperature obtained at the temperature sensor 2.

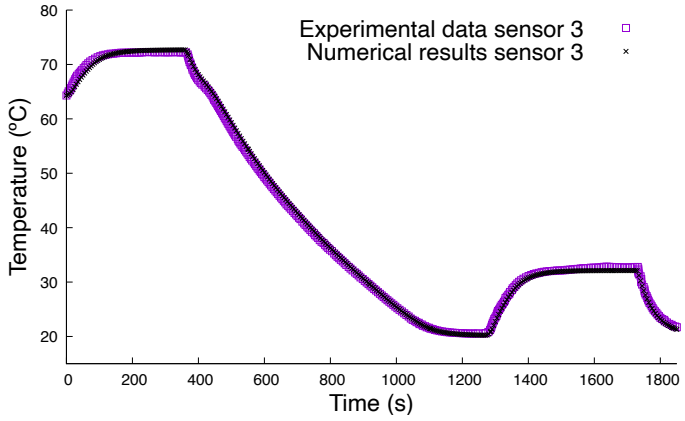

Figure 7. Comparison between the temperature obtained at the temperature sensor 3.

3. Conclusions

A fully 3D finite-volume transient model for solving conjugate heat transfer problems with the possibility of including radiation, even for semi-transparent media, has been developed. Then, it was validated using experimental data from a CPVT solar collector experiment. The model was able to correctly reproduce different behaviors, such as heat up of the system by means of radiation or cooling down processes with a maximum error of $+1.5°C$.

Acknowledgments

This work is supported by the SIMEX project (PID2022-142174OB-I00) of *Ministerio de Ciencia e Innovación* and the RETOtwin project (PDC2021-120970-I00) of *Ministerio de Economía y Competitividad*, Spain. D. Santos acknowledges a *FI AGAUR-Generalitat de Catalunya* fellowship (2022FI_B_00173), extended and financed by *Universitat Politècnica de Catalunya and Banc Santander*.

References

[1] Perelman T L 1961 *Int. J. Heat Mass Transf.* **3** 4 293-303

[2] Errera M, Moretti R, Mayeur J, Gelain M, Tessé L, Lamet J and Laroche E 2020 *Int. J. Heat Mass Transf.* **160** 120155

[3] Trias F X, Lehmkuhl O, Oliva A, Pérez-Segarra C D and Verstappen R W C P 2014 *J. Comput. Phys.* **258** 1 246-67

[4] Pascau A 2011 *Int. J. Numer. Methods Fluids* **65** 1 812-33

[5] Chorin A J 1968 *Math. Comput.* **22** 745-62

[6] Guadamund E, Chiva J, Colomer G, Farnós J, Al Mers A, Rigola J and Perez C 2017 *Proc. ISES Solar World Congress/IEA SHC Solar Heating and Cooling Conference (Abu Dhabi)* pp 2000-11

[7] Afzali H, Salmanzadeh M, Nasseriyan P, Hayati A, Cabral D, Gomes J and Karlsson B 2022 *Renew. Energ.* **181** 535-53

[8] Calise F, Palombo A and Vanoli L 2012 *Energy* **46** 1 283-94

[9] Demircan C, Cenk H, Keçebaş A, Calise F and Vicidomini M 2023 *Therm. Sci. Eng. Prog.* **38** 101664

[10] Laitinen A, Saari K, Kukko K, Peltonen P, Laurila E, Partanen J and V Vuorinen 2020 *Int. J. Heat Fluid Flow* **85** 108654

[11] Colomer G 2006 Numerical methods for radiative heat transfer, PhD thesis, Universitat Politècnica de Catalunya (UPC), Terrassa.

[12] Santos D, Trias F X, Colomer G and Pérez-Sergarra C D 2022 *Proc. 8th European Congress on Computational Methods in Applied Sciences and Engineering, ECCOMAS 2022 (Oslo)*

[13] Felsberger R, Buchroithner A, Gerl B and Wegleiter H 2020 *Energies* **13** 1-24